THE JOURNAL OF BIOLOGICAL CHEMISTRY VOL. 288, NO. 23, pp. 16882–16894, June 7, 2013
Published in the U.S.A.

Myocilin Stimulates Osteogenic Differentiation of Mesenchymal Stem Cells through Mitogen-activated Protein Kinase Signaling*[S]

Received for publication, September 26, 2012, and in revised form, April 10, 2013 Published, JBC Papers in Press, April 29, 2013, DOI 10.1074/jbc.M112.422972

Heung Sun Kwon, Thomas V. Johnson[1], and Stanislav I. Tomarev[2]

From the Section of Retinal Ganglion Cell Biology, Laboratory of Retinal Cell and Molecular Biology, National Eye Institute, National Institutes of Health, Bethesda, Maryland 20892

Background: Myocilin, a secreted glaucoma-associated protein, is detected in ocular and non-ocular tissues.
Results: Myocilin is expressed in mesenchymal stem cells (MSCs) and stimulates their differentiation into osteoblasts.
Conclusion: Myocilin-stimulated osteogenic differentiation of MSCs is associated with activation of MAP kinase signaling pathways.
Significance: Modulation of myocilin activity could potentially be targeted to improve the bone-regenerative potential of MSCs.

Myocilin is a secreted glycoprotein that is expressed in ocular and non-ocular tissues. Mutations in the *MYOCILIN* gene may lead to juvenile- and adult-onset primary open-angle glaucoma. Here we report that myocilin is expressed in bone marrow-derived mesenchymal stem cells (MSCs) and plays a role in their differentiation into osteoblasts *in vitro* and in osteogenesis *in vivo*. Expression of myocilin was detected in MSCs derived from mouse, rat, and human bone marrow, with human MSCs exhibiting the highest level of myocilin expression. Expression of myocilin rose during the course of human MSC differentiation into osteoblasts but not into adipocytes, and treatment with exogenous myocilin further enhanced osteogenesis. MSCs derived from *Myoc*-null mice had a reduced ability to differentiate into the osteoblastic lineage, which was partially rescued by exogenous extracellular myocilin treatment. Myocilin also stimulated osteogenic differentiation of wild-type MSCs, which was associated with activation of the p38, Erk1/2, and JNK MAP kinase signaling pathways as well as up-regulated expression of the osteogenic transcription factors Runx2 and Dlx5. Finally, cortical bone thickness and trabecular volume, as well as the expression level of osteopontin, a known factor of bone remodeling and osteoblast differentiation, were reduced dramatically in the femurs of *Myoc*-null mice compared with wild-type mice. These data suggest that myocilin should be considered as a target for improving the bone regenerative potential of MSCs and may identify a new role for myocilin in bone formation and/or maintenance *in vivo*.

Bone marrow-derived mesenchymal stem cells, also known as mesenchymal stromal cells or MSCs,[3] have attracted significant interest in recent years because of their potential clinical application to tissue regeneration and repair in multiple organ systems (see Refs. 1–3 for recent reviews). The relative ease of MSC isolation from bone marrow aspirates and their potential for autologous transplantation have made this cell type especially attractive for this purpose. Cultured MSCs are readily expandable and capable of differentiating along multiple lineages, including those of osteoblasts, chondrocytes, adipocytes, and myoblasts, under appropriate conditions (4, 5). Several growth factors and signaling pathways have been implicated in controlling MSC differentiation along specific lineages (6). For example, it has been suggested that differentiation of MSCs into osteoblasts may involve the integration of the bone morphogenic protein, Notch, Wnt, Hedgehog, and fibroblast growth factor signaling pathways. These pathways lead to activation of a set of transcription factors, including Runx2 and NFAT2, that regulate the expression of genes essential for osteoblast differentiation, such as collagen type 1, osteopontin, sparc, and osteocalcin (see Ref. 7 for a recent review). The translation of MSC therapy into clinical application, however, will require a more complete understanding of how signaling pathways integrate to control cell maintenance, proliferation, commitment, and differentiation.

Human myocilin is a secreted glycoprotein with a length of 504 amino acids. Mutations in the *MYOCILIN* (*MYOC*) gene are found in more than 10% of juvenile open-angle glaucoma cases and in 3–4% of patients with adult-onset primary open-angle glaucoma (8–12). *MYOC* is expressed in ocular (trabecular meshwork, iris, ciliary body, sclera, and retinal pigmented epithelial cells) and non-ocular (sciatic nerve, skeletal muscle, mammary gland, thymus, and testis) tissues. Myocilin is not known to play a role in human disease outside of the eye. How-

* This work was supported, in whole or in part, by the Intramural Research Program of the National Institutes of Health, National Eye Institute.
[S] This article contains supplemental Figs. S1 and S2.
[1] Present address: School of Medicine, Johns Hopkins University, Baltimore, MD.
[2] To whom correspondence should be addressed: Building 6, Room 212, 6 Center Dr., SRGCB, LRCMB, National Eye Institute, National Institutes of Health, Bethesda, MD 20892. Tel.: 301-496-8524; Fax: 301-480-2610; E-mail: tomarevs@nei.nih.gov.

[3] The abbreviations used are: MSC, mesenchymal stem cell; hMSC, human mesenchymal stem cell; mMSC, mouse mesenchymal stem cell; AP, alkaline phosphatase; qRT-PCR, quantitative real-time PCR; micro-CT, micro-computed CT.

ever, we have demonstrated recently that overexpression of wild-type myocilin in transgenic mouse skeletal muscle leads to increased muscle size and suggested that myocilin may regulate muscle hypertrophy (13). We have also shown that myocilin may serve as a modulator of Wnt signaling by interacting with several Wnt receptors, frizzled receptors, and antagonists of Wnt, including Wif-1 and sFRP (secreted Frizzled-related) proteins (14). In the experimental models we used, myocilin stimulated noncanonical but not canonical Wnt signaling pathways. Treatment of different cell types with extracellular myocilin induces formation of stress fibers and intracellular redistribution of β-catenin with accumulation on the cellular membrane but not in cell nuclei (14).

Here we demonstrate that myocilin is expressed in MSCs and plays a role in MSC differentiation along the osteoblastic lineage. MSCs exhibit an increase in myocilin expression when cultured in osteogenic conditions, and addition of exogenous myocilin increases the efficiency of osteogenic differentiation in wild-type MSC cultures. MSCs isolated from the bone marrow of *Myoc*-null mice have an impaired ability to differentiate along the osteoblastic lineage, but addition of exogenous myocilin improves osteogenic differentiation in MSC cultures from these mice. Stimulation of MSC differentiation into osteoblasts by extracellular myocilin is associated with activation of the p38, Erk1/2, and JNK MAPK signaling pathways, and blocking these pathways attenuates osteogenic differentiation by MSCs. We also speculate that myocilin may play a role in osteogenesis more generally because *Myoc*-null mice exhibit reduced cortical bone thickness and trabecular volume compared with wild-type mice.

EXPERIMENTAL PROCEDURES

Animals—Mice (B6/129 mixed background) and Sprague-Dawley rats were maintained in accordance with the guidelines set forth by the National Eye Institute Committee on the Use and Care of Animals. *Myoc*-null mice have been described previously (15).

Cell Cultures—Human MSCs (hMSCs) were purchased from the ATCC and grown according to the instructions of the manufacturer. Rat MSCs were isolated from femoral bone marrow aspirates as described previously (16). Mouse MSCs (mMSCs) were isolated from femoral bone marrow aspirates of wild-type and *Myoc*-null mice as described previously (17). In brief, 6-week-old rats or mice were sacrificed by increasing exposure to CO_2 followed by cervical dislocation. The body of the animal was rinsed in 70% ethanol, and the cutaneous tissues were removed. Lower limbs were disarticulated and stored briefly on ice in DMEM supplemented with penicillin (100 units/ml) and streptomycin (100 μg/ml). Bone marrow was aspirated from femurs by flushing them with 1–2 ml of DMEM. Mononucleated cells from the bone marrow were plated at 2×10^7 cells/100 mm^2 on plastic culture dishes in DMEM supplemented with 10% FBS and penicillin (100 units/ml) and streptomycin (100 μg/ml) at 37 °C in 5% CO_2. Non-adherent cells were removed after 48–72 h, and adherent cells (MSCs) were replenished with fresh medium every 2–3 days until confluent. MSCs between passages 7 and 9 were used in all experiments.

Cell Differentiation—MSCs were seeded into culture vessels at 5×10^3 cells/cm^2. For osteogenic differentiation, the cultures were incubated in osteoblast differentiation medium (StemPro osteogenesis differentiation kit, Invitrogen) for up to 3 weeks. The medium was changed two times per week. The cells were fixed with 10% formalin for 20 min at room temperature and stained with Alizarin Red S (pH 4.1) (Sigma) for 20 min at room temperature. For adipogenic differentiation, the cultures were incubated in adipocyte differentiation medium (StemPro adipogenesis differentiation kit, Invitrogen) for 3 weeks. The medium was changed twice weekly. The cells were then fixed with 10% formalin for 20 min at room temperature and stained with 0.5% Oil Red O (Sigma) in methanol (Sigma) for 20 min at room temperature. Alkaline phosphatase (AP) activity assays were carried out by washing cells in PBS and lysing them with three cycles of freezing and thawing in 0.05% Triton X-100. An aliquot of the lysate was incubated with naphthol AS-MX phosphate alkaline solution with fast blue RR salt at 37 °C for 30 min. The reactions were stopped by adding 5 μl of 2 M NaOH to 50 μl of extracts, and the absorbance was measured at 405 nm using a multifunctional reader (Bio-Rad). AP activity was normalized to total protein concentration, which was determined using Bradford reagent (Bio-Rad). For chondrocyte differentiation, the cultures were incubated in chondrocyte differentiation medium (StemPro chondrogenesis differentiation kit, Invitrogen) for 2 weeks. The medium was changed every 2–3 days. MAP kinase inhibitors SB203580 and SP600125 (Sigma-Aldrich), BIRB 796 (Selleck Chemicals LLC, TX) and BI 78D3 (R&D Systems, MN) were prepared and used as recommended by the manufacturers. Si-JNK#1 (5′-GGAGCUCAAGGAAUAGUAU-3′), si-p38#1 (5′-GCCCAUAAGGCCAGAAACU), and control scrambled si-S1 siRNA oligonucleotides (Cell Signaling Technology, Inc., MA) were used at a final concentration of 10 and 100 nM. Si-p38#2 (GCCCUGAGGUUCUGGCAA); si-p38#3 (CGACGAGCACGUUCAAUUC); si-p38#4 (CCAUAGACCUCCUUGGAAG); si-JNK#2 (GCCCAGUAAUAUAGUAGUA); si-JNK#3 (GGCAUGGGCUACAAGGAAA); si-JNK#4 (GAAUAGUAUGCGCAGCUUA); and the non-targeting pool of control si-S2 (5′-UGGUUUACAUGUCGACUAA-3′, 5′-UGGUUUACAUGUUGUGUGA-3′, 5′-UGGUUUACAUGUUUUCUGA-3′, and 5′-UGGUUUACAUGUUUUCCUA-3′) siRNAs (Dharmacon, CO) were used at final concentration of 100 nM. hMSCs were transfected using siLentFect (Bio-Rad) according to the instructions of the manufacturer 4 days after the beginning of osteoblastic differentiation.

Quantitative Real-time PCR (qRT-PCR)—Total RNA was extracted from cell cultures using the RNeasy mini kit (Qiagen, Valencia, CA). Human muscle RNA was purchased from ORIGENE (Rockville, MD). 20 ng of RNA were used for each qRT-PCR reaction. qRT-PCR was performed using the SuperScript® III one-step qRT-PCR system with Platinum® Taq kit according to the instructions of the manufacturer (Invitrogen). Primers for qRT-PCR were as follows: human *MYOC,* 5′-ATTTGAAGGAGAGCCCATC-3′ and 5′-GCTACCCCTTCTAAGGTTCAC-3′; human *GAPDH*, 5′-ACCCATCACCATCTTCCAGGAGCG-3′ and 5′-CGGGAAGCTCACTGGCATGGCCT-3′; mouse *Dlx5*, 5′-CCAACCAGCCAGAGAAA-

GAA-3′ and 5′-GCAAGGCGAGGTACTGAGTC-3′; mouse *Runx2*, 5′-AACCCACGAATGCACTATCCA-3′ and 5′-CGGACATACCGAG GGACATG-3′; mouse osteocalcin, 5′-AGCAAAGGTGCAGCCTTTGT-3′ and 5′-GCGCCTGGGTCTCTTCACT-3′; and mouse *Gapdh*, 5′-CCCATCACCATCTTCCAGGAGCG-3′ and 5′-CGGGAAGCTCACTGGCATGGCCT-3′. GAPDH was used for normalization. qRT-PCR was carried out on a 7900HT real-time thermocycler (Applied Biosystems, CA). Control experiments showed that the efficiency of amplification was very similar for different primer sets (less than 5% difference). To quantifying the relative changes in gene expression, we used the $2^{-\Delta\Delta C_T}$ method. The average C_T was calculated for the target genes and internal control (*GAPDH*), and the ΔC_T ($C_{T,target}$-$C_{T,GAPDH}$) values were determined. All reactions were performed in triplicate using three independent samples.

Western Blot Analysis—Cells were washed once with PBS and then lysed in lysis buffer containing 1% Nonidet P-40, 5% sodium deoxycholate, 1 mM phenylmethylsulfonyl fluoride, 100 mM sodium orthovanadate, and 1:100 protease inhibitor mixtures (Sigma). 5- to 10-μg aliquots of protein extracts were separated by 4–12% SDS-PAGE and transferred to polyvinylidene difluoride membranes (Invitrogen). The membranes were blocked with 5% nonfat milk overnight at 4 °C and then probed with primary antibodies. The immunocomplexes were visualized with horseradish peroxidase-coupled goat anti-rabbit or anti-mouse IgG (GE Healthcare, NJ) using SuperSignal reagents (Pierce). Primary antibodies used were as follows: anti-phosphorylated JNK and anti-total JNK monoclonal antibodies (Sigma); anti-HSC70 monoclonal antibodies (Santa Cruz Biotechnology, Inc., CA); anti-Runx2 (Millipore, MA); anti-Dlx5 (Chemicon, CA); anti-phospho-p38 polyclonal and anti-p38 (Cell Signaling Technology, Inc.); and anti-phospho-Erk1/2, anti-Erk1/2, and anti-PPARγ (Cell Signaling Technology, Inc.). Antibodies against myocilin have been described previously (18). For digital quantification, membranes were scanned using a Typhoon 9410 variable-mode imager (Amersham Biosciences) and analyzed using Image Scion Alpha 4.0.3.2 (Scion Cor, Frederick, MD). In some cases, the chemiluminescent signals were captured using an 8-megapixel scientific-grade CCD camera (Flurochem M., Santa Clara, CA), and the signal intensities were quantified and analyzed using AlphaView software (Proteinsimple, Santa Clara, CA). All experiments were repeated at least twice.

Immunofluorescence—MSCs were seeded on 2-well glass chamber slides (Nalge Nunc, NY) and cultured for 24 h in complete DMEM. The medium was removed, and cells were washed 2–3 times with PBS. The MSCs were fixed with fresh 3.7% formaldehyde for 10 min at room temperature and permeabilized with 0.1% Triton X-100 in PBS for 5 min. After blocking with 5% BSA in PBS at room temperature for 1 h, cells were incubated with anti-myocilin (1:500 dilution) polyclonal and anti-golgin-97 monoclonal antibody (1:200) (Invitrogen) or anti-protein-disulfide isomerase monoclonal antibody (1:200 dilution) (Abcam, Cambridge, MA) at room temperature for 1 h. Cells were washed with PBS-Tween 20 and then incubated with Alexa Fluor 488- or 594-conjugated secondary antibodies for 30 min. An Axioplan 2 fluorescent microscope and Zeiss 700 confocal microscope (Carl Zeiss MicroImaging, Inc. NY) were used to detect fluorescence. The images were processed with Adobe Photoshop Elements 2.0 (Adobe Inc., CA). Identical processing parameters were used for all images within any single experiment. p-p38 detection was performed with polyclonal anti-phosphorylated p38 antibody (1:100) (Cell Signaling Technology, Inc.) and revealed with secondary Alexa Fluor 569 anti-mouse antibody (1:500) (Invitrogen). DAPI (Sigma) was used for counterstaining. Anti-osteopontin (1:200) and anti-CD106 (1:200) antibodies (R&D Systems) were used as primary antibodies for immunostaining of frozen sections of the femurs.

Micro-CT Scanning—Mouse femurs were removed from alcohol storage and dried superficially on paper tissue before being wrapped in parafilm to prevent drying during scanning. Each parafilm-wrapped femur ($n = 3$ for each group) was placed in a plastic/polystyrene foam tube that was mounted vertically in the scanner. Micro-CT of mouse anatomy was performed with a SkyScan 1172 Micro x-ray CT scanner (Micro Photonics, Inc., Allentown PA) with the x-ray source (focal spot size, 4 μm, energy range 20–100 kV) biased at 50 kV/200 microamps and with a 0.5 A mm filter to reduce beam hardening. The images were acquired with a pixel size of 6.87 μm with the camera-to-source distance of 221.553 mm and an object-to-source distance of 65.935 mm. 799 projections were acquired with an angular resolution of 0.4 degrees through 180 degrees of rotation. Four frames were averaged for each projection radiograph with an exposure time of 295 ms/frame. The scan duration was ~30 min/femur. Tomographic images were reconstructed using vendor-supplied software on the basis of the Feldkamp cone beam algorithm.

Statistical Analysis—Quantitative data are expressed as mean ± S.E. Two-tailed Student's *t* tests were used where comparisons between two groups were made. One-way analyses of variance with Bonferroni multiple comparisons post hoc tests (only computed if overall $p < 0.05$) were used when comparisons of three or more treatment groups were made (IBM SPSS Statistics 17).

RESULTS

Myocilin Is Expressed in Mouse, Rat, and Human MSCs—Available data suggest that the mouse *Myoc* gene is expressed highly in joint tissues. Because cultured MSCs are capable of differentiating into chondrocytes under appropriate conditions (19, 20), we examined whether myocilin is also present in MSCs. Myocilin protein was detected in mouse, rat, and human MSCs, with hMSCs demonstrating the highest levels of myocilin antibody reactivity (Fig. 1, *A* and *B*). The level of myocilin in mMSCs was about 4-fold lower than in mouse skeletal muscles, a tissue known to express relatively high levels of myocilin (13, 21). Similarly, the level of *MYOC* mRNA in hMSCs was about 2-fold lower than in human skeletal muscles as judged by qRT-PCR analysis (Fig. 1*C*). Immunostaining of hMSCs demonstrated that myocilin was located preferentially in the endoplasmic reticulum and Golgi apparatus (Fig. 1, *D* and *E*), similar to its localization in trabecular meshwork cells (18, 22).

Myocilin was discovered as a protein that is induced by glucocorticoids in the ocular trabecular meshwork (23). Likewise, we found that myocilin could be induced by glucocorticoids in

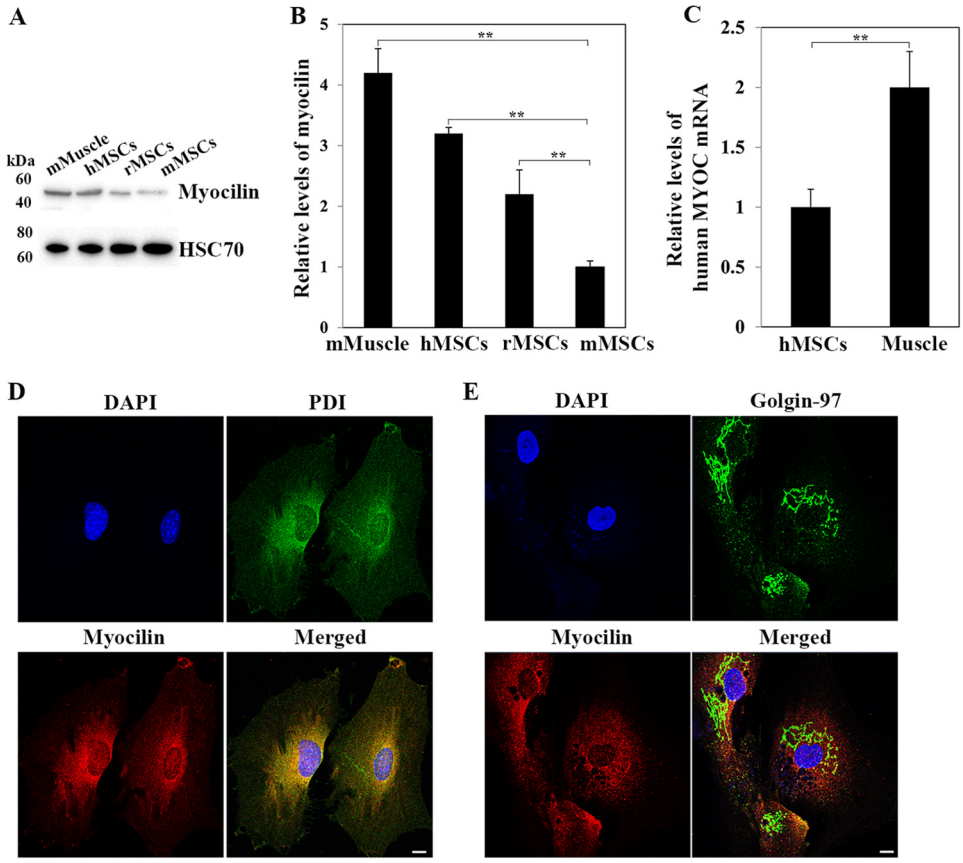

FIGURE 1. **Myocilin expression in MSCs from different species.** *A*, Western blot analysis of myocilin in lysates of MSCs from different species. Mouse skeletal muscle (*mMuscle*) was used as a positive control. Lysates were probed with polyclonal antibodies against mouse myocilin (1:2000). *B*, quantification of three independent Western blot experiments with the mean level of myocilin expression in mMSCs taken as one arbitrary unit. **, $p < 0.01$. *C*, relative levels of *MYOC* mRNA in hMSCs and human muscle as judged by qRT-PCR analysis. GAPDH mRNA was used for normalization. The mean level of *MYOC* expression in hMSCs was taken as one arbitrary unit. **, $p < 0.01$. *D* and *E*, intracellular distribution of myocilin in hMSCs. Cells were stained with antibodies against mouse myocilin (*red*) and antibodies against protein-disulfide isomerase (*PDI*) or golgin-97 (*green*). Nuclei were stained with DAPI (*blue*). The merged images demonstrate colocalization with endoplasmic reticulum (*D*) and Golgi markers (*E*). Typical immunofluorescence patterns are shown. *Scale bar* = 10 μm.

MSCs with kinetics typical for an indirectly responsive glucocorticoid-inducible gene (23, 24). The level of myocilin induction was more than 2-fold at 4 days and more than 4-fold at 8 days following addition of 100 nM dexamethasone (Supplemental Fig. S1, *A* and *B*). To test whether MSC differentiation is associated with changes in myocilin expression, we compared myocilin levels in the lysates of undifferentiated hMSCs and hMSC cultured in chondrogenic, adipogenic, or osteogenic conditions. Myocilin levels were increased by more than 2-fold in hMSCs differentiating into osteoblasts as compared with undifferentiated hMSCs or hMSCs differentiating into chondrocytes or adipocytes (Fig. 2, *A–D*). The levels of *MYOC* mRNA were also increased about 2-fold in hMSCs differentiating into osteoblasts as compared with undifferentiated hMSCs or hMSCs differentiating into adipocytes (Fig. 2*E*). In summary, these results demonstrate that myocilin is expressed in MSCs and that its level increases when these cells differentiate into osteoblasts.

Extracellular Myocilin Enhances Osteogenic Differentiation of MSCs—Myocilin is a secreted glycoprotein that may interact with frizzled receptors on the cell surface (14) and with extracellular proteins (25, 26). Because the expression of myocilin was increased in MSCs differentiating into osteoblasts, we tested whether treatment with extracellular myocilin might affect MSC osteogenesis. Addition of myocilin (3 μg/ml) to hMSCs did not affect their differentiation into adipocytes as judged by Oil Red O staining and PPARγ expression (Fig. 3, *A–D*), but stimulated their differentiation into osteoblasts as evaluated by Alizarin Red S staining (Fig. 3, *E* and *F*). Moreover, the effect of exogenously applied myocilin on MSC osteogenesis was dose-dependent through a range of 1–3 μg/ml, as judged by Alizarin Red S staining and measurements of AP activity (Fig. 4*A*). Higher tested concentrations of exogenous myocilin ($\geq$ 6 μg/ml) did not lead to further elevation of AP activity compared with 3 μg/ml of myocilin (Fig. 4*A*), so we used 3 μg/ml of myocilin in most subsequent experiments. Addition of antiserum against myocilin (1:1000 dilution) simultaneously with myocilin eliminated the pro-osteogenic effect of myocilin (Fig. 4*A*).

To determine whether the presence of endogenous myocilin contributes to osteoblastic differentiation by MSCs, we compared differentiation of mMSCs from wild-type and *Myoc*-null mice. As judged by AP activity measurements, mMSCs from *Myoc*-null mice demonstrated less osteogenesis when cultured in osteoblast differentiation medium (Fig. 4*B*). Addition of myocilin (1–3 μg/ml) to differentiating mMSCs from *Myoc*-null mice led to elevation of AP activity in a dose-dependent manner but with higher concentrations of myocilin (6 μg/ml)

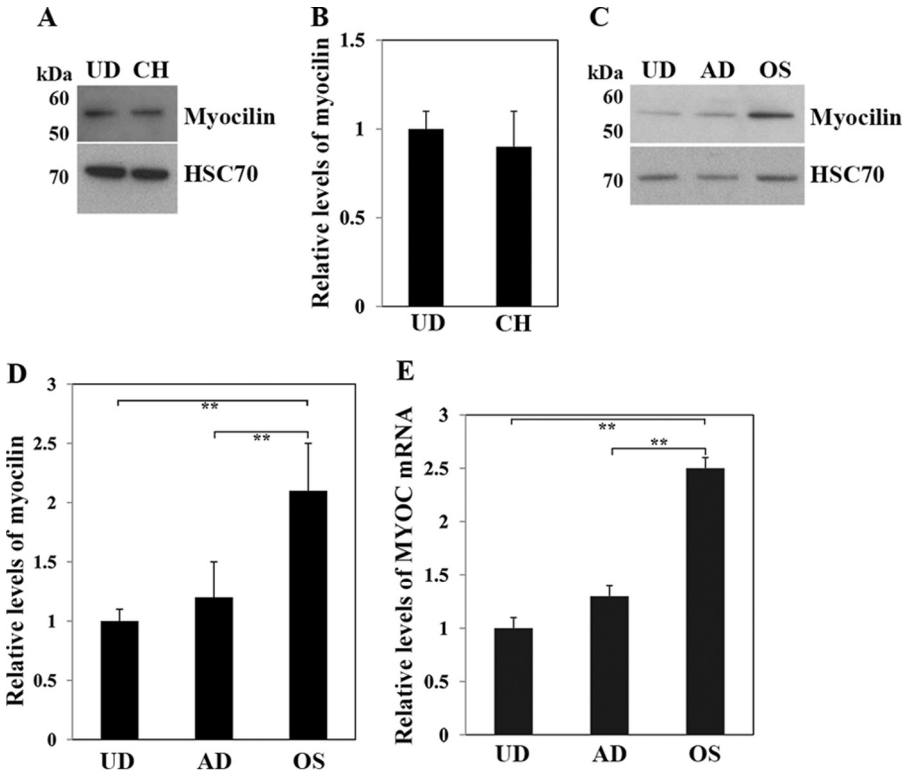

FIGURE 2. **Changes in myocilin protein and *MYOC* mRNA in the course of MSC differentiation along the chondrogenic, adipogenic, and osteogenic lineages.** *A*, Western blot analysis of myocilin in the lysates of undifferentiated (*UD*) hMSCs and hMSCs differentiating into chondrocytes (*CH*) after 2 weeks. Equal amounts of lysates were probed with antibodies against myocilin (1:2000) and HSC70 (1:5000). *B*, quantification of three independent Western blot experiments with the mean level of myocilin expression in undifferentiated hMSCs taken as one arbitrary unit. *, $p < 0.05$; **, $p < 0.01$. *C*, Western blot analysis of myocilin in the lysates of undifferentiated hMSCs and hMSCs differentiating into adipocytes (*AD*) or osteoblasts (*OS*) after 6 days. Equal amounts of lysates were probed with antibodies against myocilin (1:2000) and HSC70 (1:5000). *D*, quantification of three independent Western blot experiments with the mean level of myocilin expression in undifferentiated hMSCs taken as one arbitrary unit. **, $p < 0.01$. *E*, relative levels of *MYOC* mRNA in undifferentiated and differentiating hMSCs as judged by qRT-PCR analysis. hMSCs were differentiated for 4 days. *GAPDH* was used for normalization. The level of *MYOC* expression in undifferentiated hMSCs was taken as one arbitrary unit. **, $p < 0.01$.

showing reduced stimulatory effects compared with the peak effect at 3 μg/ml. The maximal level of myocilin-mediated stimulation of relative AP activity in *Myoc*-null mMSCs (~4-fold) was lower than that for wild-type mMSCs (~8-fold, Fig. 4, *A–C*).

Myocilin Enhances Osteogenic Differentiation of hMSCs through the p38 MAPK and JNK Signaling Pathways—Several signaling pathways have been implicated in the regulation of MSC osteoblastic differentiation (7). Although myocilin may serve as a modulator of Wnt signaling, *in vitro* experiments studying effects of canonical and noncanonical Wnt signaling on osteogenesis have been inconclusive (7). Therefore, we sought to determine how myocilin affects other signaling pathways with known involvement in osteogenesis by osteoblasts and/or MSCs, such as the JNK and p38 MAPK pathways (27, 28). Addition of myocilin (3 μg/ml) simultaneously with osteoblast differentiation medium to hMSCs increased the levels of activated p38 (p-p38), activated JNK (p-JNK), and activated Erk1/2 (p-Erk1/2, a downstream mediator of MAPK signaling) measured 1 h after initiation of differentiation (Fig. 5, *A–F*). Addition of the inhibitors of p38 (SB203580) (29, 30) or JNK (SP600125) (31) eliminated the stimulating effects of myocilin (Fig. 5, *A–D*). Although SB203580 and SP600125 have been utilized throughout the published literature as specific inhibitors of p38 and JNK, respectively, it has been reported that they may have additional targets (32). To address the issue of inhibitor specificity, we employed another set of inhibitors, BIRB 796 (32, 33) and BI 78D3 (34), that act by mechanisms that are different from SB203580 and SP600125. Similar to the results with SB203580 and SP600125, treatment with alternative inhibitors of p38 (BIRB 796) or JNK (BI 78D3) significantly reduced the stimulating effects of myocilin, as measured 1 h after initiation of differentiation (Fig. 6, *A–C*).

Prolonged exposure (6 days) of hMSCs to myocilin in the course of their differentiation into osteoblasts produced similar effects on MAPK activation (data not shown). The levels of p-p38, p-JNK, and p-Erk1/2 were increased about 4-, 2-, and 2.5-fold, respectively, compared with hMSCs that were differentiated in the absence of myocilin, whereas addition of antiserum against myocilin together with myocilin completely eliminated a stimulating effect of myocilin, confirming the specificity of myocilin action (Figs. 7 and 8). Myocilin treatment led to migration of activated p38 to the nucleus, whereas addition of antiserum against myocilin prevented accumulation of p-p38 in the nucleus (Fig. 7*C*). Addition of SB203580 or SP600125 completely eliminated or significantly reduced the osteogenesis-stimulating effects of myocilin, as judged by Alizarin Red S staining and AP assays (Figs. 7, *D* and E, and 8*E*). As an alternative method of suppressing p38 and JNK we used siRNAs. Transfection of hMSCs with 100 nM of different p38

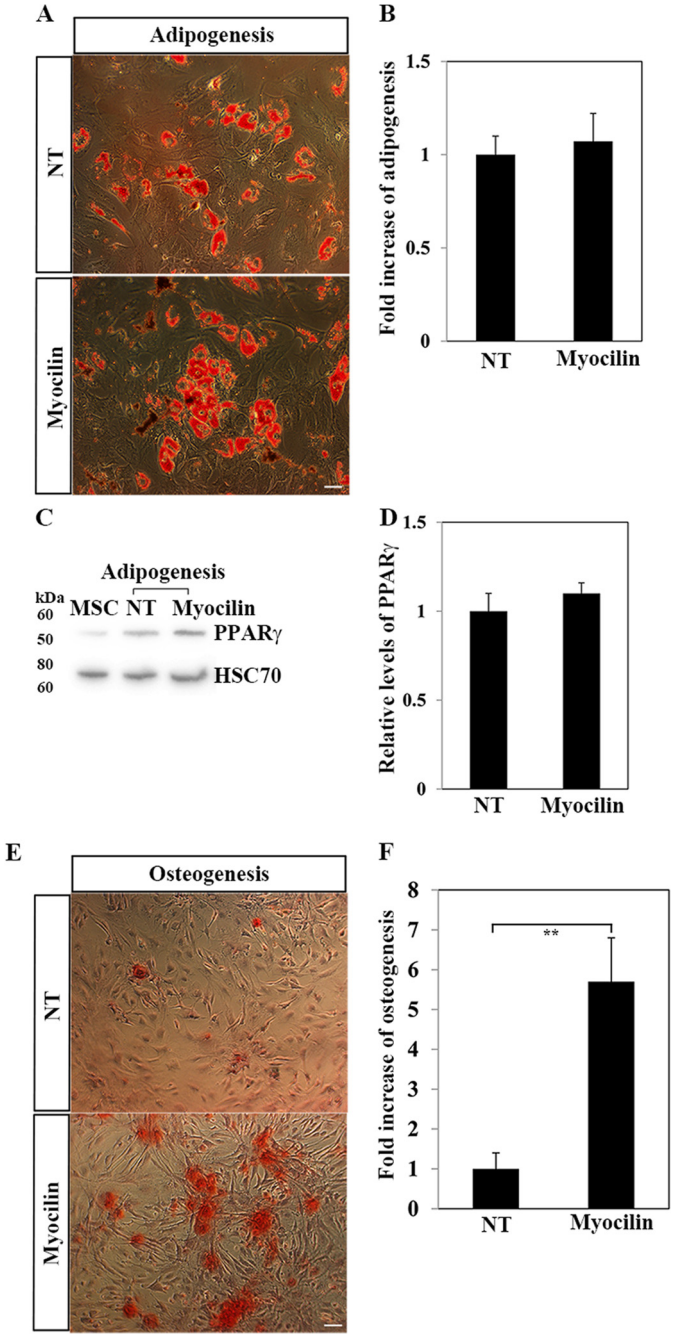

FIGURE 3. **Effects of exogenous myocilin on hMSC differentiation along the adipogenic and osteogenic lineages.** hMSCs were cultured for 6 days in adipogenic (*A*) or osteogenic (*E*) medium with or without addition of myocilin (3 μg/ml) and stained with Oil Red O or Alizarin Red S, respectively. *NT*, no treatment. *B* and *F*, quantification of the results shown in *A* and *E*. Four wells were counted per condition. The average number of cells counted per well was 350 and 470 in *A* and *E*, respectively. For statistical analysis, Student's *t* tests compared the average proportion of differentiated cells/well between the treatment and control groups, with $n = 4$ wells/group in each experiment. **, $p < 0.01$. *Scale bar* = 10 μm. *C*, Western blot analysis of the adipocyte marker *PPARγ* in the lysates of undifferentiated hMSCs (*MSC*) or hMSCs differentiating into adipocytes for 6 days in the absence (*NT*) or presence of myocilin (3 μg/ml). Equal amounts of lysates were probed with antibodies against PPARγ (1:2000) and HSC70 (1:5000). *D*, quantification of three independent Western blot experiments is shown, with the mean level of myocilin expression in undifferentiated hMSCs taken as one arbitrary unit.

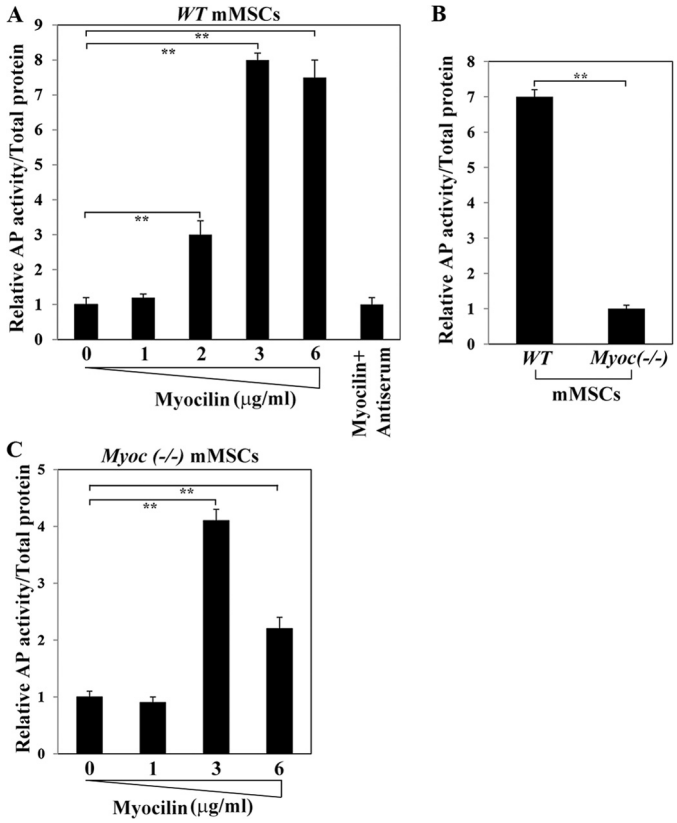

FIGURE 4. **Dose dependence of myocilin in promoting osteogenesis in mMSCs from wild-type and *Myoc*-null mice.** *A*, relative AP activity in mMSC culture lysates after cultivation of mMSCs in the presence of osteogenic induction medium plus increasing myocilin concentrations for 6 days. The level of AP activity in untreated mMSCs was taken as one arbitrary unit. **, $p < 0.01$. *B*, relative AP activity in mMSCs from wild-type and *Myoc*-null mice. AP activity was measured 6 days after initiation of osteoblastic differentiation. *C*, relative AP activity in *Myoc*-null mMSC culture lysates after cultivation of mMSCs in osteogenic differentiation medium and in the presence of increasing myocilin concentrations for 6 days. The level of AP activity in untreated mMSCs was taken as one arbitrary unit. Each *panel d*epicts quantification of three independent experiments. **, $p < 0.01$.

siRNAs or JNK siRNAs 4 days after initiation of differentiation significantly reduced the levels of p38 or JNK, respectively, 48 h after transfection (supplemental Fig. S2, *A–D*). We selected two different p38 siRNAs and two different JNK siRNAs for subsequent experiments. Transfection of hMSCs with p38 or JNK siRNAs, but not with scrambled siRNAs, reduced the stimulatory effect of myocilin (3 μg/ml) on osteogenic differentiation, as judged by AP activity measurements 6 days after initiation of differentiation (supplemental Fig. S2*E*). The inhibitory effects of siRNAs were less pronounced than the ones observed with specific inhibitors of p38 and JNK. This may be due to the fact that siRNAs were present only during last 48 h of differentiation of hMSCs into osteoblasts.

MSC osteogenesis involves many steps controlled by a hierarchy of transcription factors. Molecular and genetic studies have established a critical role for the Runx2 transcription factor in osteogenesis (35). Another important transcription factor that is involved in osteoblastic differentiation and may operate up-stream of Runx2 is Dlx5 (36). We measured mRNA levels for these transcription factors as well as for a late and specific marker of bone formation, osteocalcin, in mMSCs isolated from wild-type and *Myoc*-null mice that were differenti-

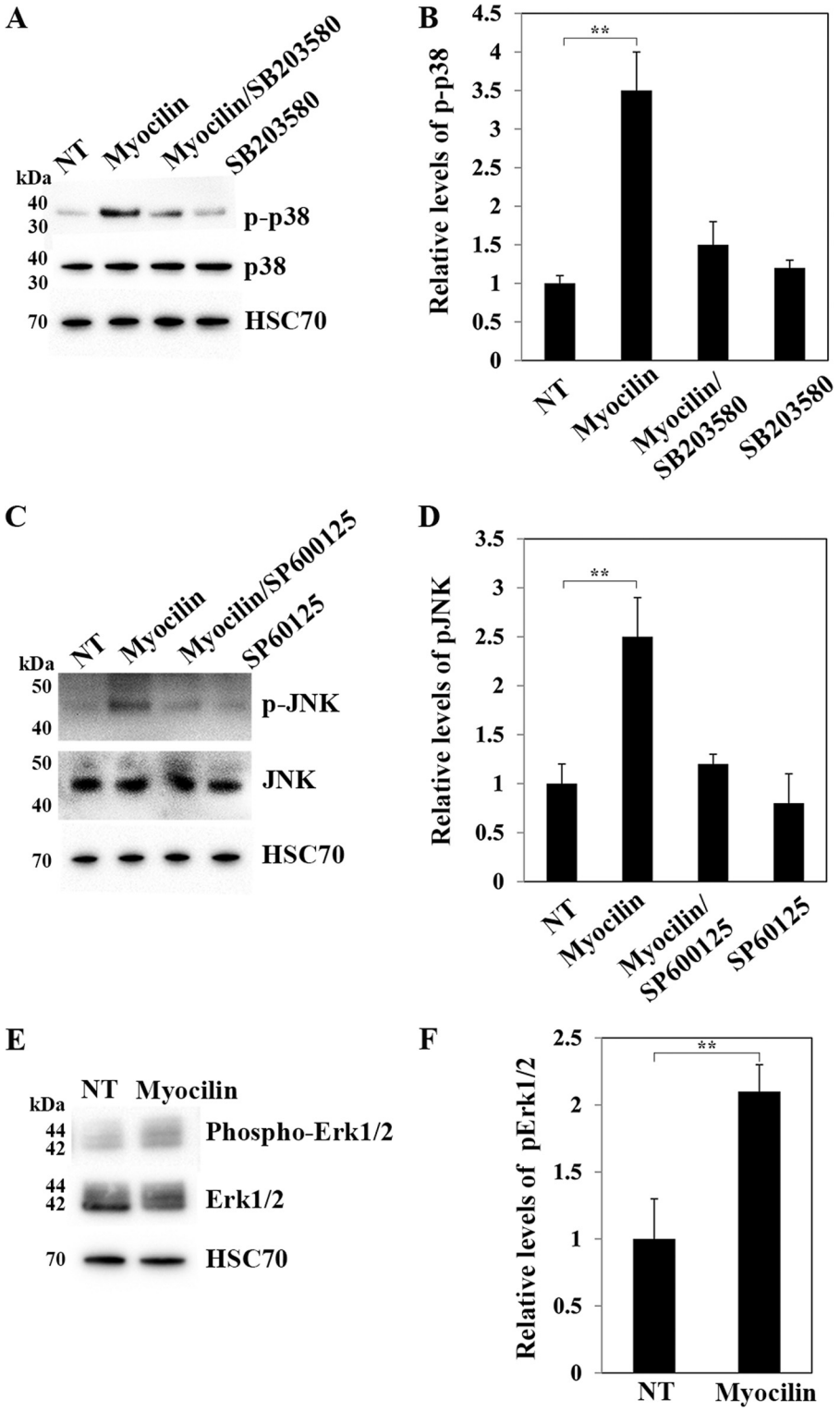

FIGURE 5. **Myocilin-induced activation of the p38, JNK, and ERK signaling pathways.** *A*, Western blot analysis of phosphorylated p38 (p-p38) levels in hMSCs differentiating into osteoblasts for 1 h in the absence (no treatment, *NT*) or presence of myocilin (3 μg/ml). SB203580 (10 μM), a specific inhibitor of p38, was added where shown. *B*, quantification of three independent Western blot experiments with the mean level of p-p38 normalized to total p38 in hMSCs differentiating without myocilin (*NT*) taken as one arbitrary unit. **, $p < 0.01$. *C*, Western blot analysis of phosphorylated JNK (*p-JNK*) levels in hMSCs differentiating into osteoblasts for 1 h in the absence (*NT*) or presence of myocilin (3 μg/ml). SP60125 (20 μM), a specific inhibitor of JNK, was added where shown. *D*, quantification of three independent Western blot experiments with the mean level of p-JNK normalized to total JNK in hMSCs differentiating without myocilin (*NT*) taken as one arbitrary unit. **, $p < 0.01$. *E*, Western blot analysis of phosphorylated Erk1/2 (*p-Erk1/2*) levels in hMSCs differentiating into osteoblasts for 1 h in the absence (*NT*) or presence of myocilin (3 μg/ml). *F*, quantification of three independent Western blot experiments with the mean level of p-Erk1/2 normalized to total Erk1/2 in hMSCs differentiating without myocilin taken as one arbitrary unit. **, $p < 0.01$. HSC70 was used for normalization in all experiments.

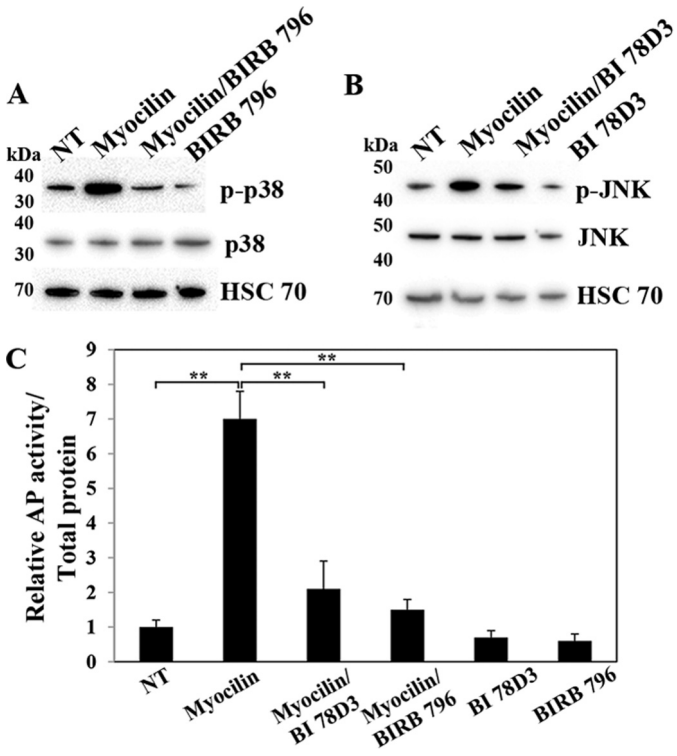

FIGURE 6. **Inhibition of myocilin-induced activation of p38 and JNK as well as osteogenic differentiation by BIRB 796 and BI 78D3.** Western blot analysis of phosphorylated p38 (*p-p38*) (*A*) and p-JNK (*B*) levels in hMSCs differentiating into osteoblasts for 1 h in the absence (no treatment, *NT*) or presence of myocilin (3 μg/ml). BIRB 796 (250 nM), a specific inhibitor of p38, and BI 78D3 (10 nM), a specific inhibitor of JNK, were added where shown. HSC70 was used for normalization in all experiments. *C*, relative AP activity in hMSCs measured 6 days after initiation of osteoblastic differentiation in the presence of myocilin (3 μg/ml), BIRB 796 (250 nM), and BI 78D3 (10 nM) is shown. Quantification of three independent experiments is shown, with the mean level of AP activity in hMSCs differentiating without myocilin (*NT*) taken as one arbitrary unit. **, $p < 0.01$.

ating into osteoblasts in the presence or absence of myocilin for 4 days. The level of *Dlx5* mRNA was higher, whereas the levels of *Runx2* and osteocalcin mRNAs did not differ significantly in MSCs from wild-type mice compared with MSCs from *Myoc*-null mice differentiating in the absence of Myocilin treatment (Fig. 9*A*). The levels of *Dlx5* and *Runx2* mRNAs were elevated in mMSCs from both wild-type and *Myoc*-null mice differentiating into osteoblasts in the presence of myocilin compared with without myocilin treatment, although the rise in expression of these factors was blunted in *Myoc*-null mMSCs compared with WT mMSCs. The levels of osteocalcin mRNA did not change significantly as a result of myocilin treatment after 4 days. Osteocalcin is a late osteogenic differentiation marker as compared with Dlx5 and Runx2, and longer myocilin treatment is probably necessary to produce elevated levels of osteocalcin. Addition of antibodies against myocilin eliminated the stimulating effect of myocilin on Runx2 and Dlx5 expression. The levels of Runx2 and Dlx5 proteins were also increased in hMSCs differentiating into osteoblasts after treatment with myocilin (Fig. 9*B*). Thus, it appears that myocilin stimulates the osteogenic differentiation of MSCs by activating osteogenic transcription factors that potentially lie downstream of the JNK and p38 MAP kinase pathways.

Reduction of Cortical Bone Thickness in Myoc-null Mice—The impaired ability of mMSCs from *Myoc*-null mice to differentiate into osteoblasts in culture suggested that this may correlate with defects in bone formation in these mice compared with wild-type littermates. As the first step to test this hypothesis, we immunostained frozen sections of the femur bone marrow from wild-type and *Myoc*-null mice with antibodies against osteopontin and CD106, a positive marker for mouse MSCs. A significant decrease in the staining intensity was observed for both markers (Fig. 10, *A* and *B*). Subsequently, we employed microcomputed tomography (micro-CT) to characterize the three-dimensional trabecular and cortical bone structures of wild-type and *Myoc*-null mouse femurs. The results showed that cortical bone thickness (Fig. 10, *E* and *F*) as well as trabecular volume (*C* and *D*) were reduced in the *Myoc*-null mice compared with wild-type mice. These data suggest that myocilin plays a role in bone formation and/or maintenance *in vivo*.

DISCUSSION

Although several major signaling pathways have been implicated in the differentiation of MSCs into osteoblasts (7), the mechanisms controlling osteogenic differentiation are still not well understood. In this work we demonstrate that myocilin is expressed in MSCs and identify myocilin as a novel molecular participant in the differentiation of MSCs into osteoblasts.

Myocilin was originally identified as a protein that was highly induced by glucocorticoids in human trabecular meshwork cells *in vitro*. There are only a few cell types that express myocilin in culture, and myocilin is not induced by glucocorticoids in cell lines that do not express myocilin. Myocilin expression in MSCs and its inducibility by glucocorticoids suggest that these cells would serve as a reasonable model to study regulation of the *MYOC* gene. The trabecular meshwork is a part of the aqueous humor outflow pathway located at the angle of the anterior chamber of the eye. In humans, the trabecular meshwork is made up of collagen beams covered by endothelial-like cells. The space between the beams is filled with extracellular material/matrix. Microarray analysis of gene expression has demonstrated that some genes essential for cartilage and bone formation, such as matrix Gla protein and osteopontin, are also abundantly expressed in the trabecular meshwork (37, 38). These observations led to a suggestion that calcification of the trabecular meshwork may occur in certain conditions (see (39) for review). Mutations in the *MYOC* gene may lead to glaucoma. Although the exact mechanisms are still not clear, it has been suggested that accumulation of mutated myocilin induces the unfolded protein response, makes cells more sensitive to oxidative stress, and, consequently, leads to deterioration of trabecular meshwork function and/or trabecular meshwork cell death (40–42). At the same time, no other phenotypes have been reported in humans carrying *MYOC* mutations or in mice expressing mutated myocilin (43–45). *Myoc*-null mice appeared to be normal and do not develop glaucoma, but careful analysis of non-ocular phenotypes have not been performed. Our recent data demonstrated that the absence of myocilin led to a moderate reduction in the amount of syntrophin associated with dystrophin and reduced levels of phospho-Akt in the skel-

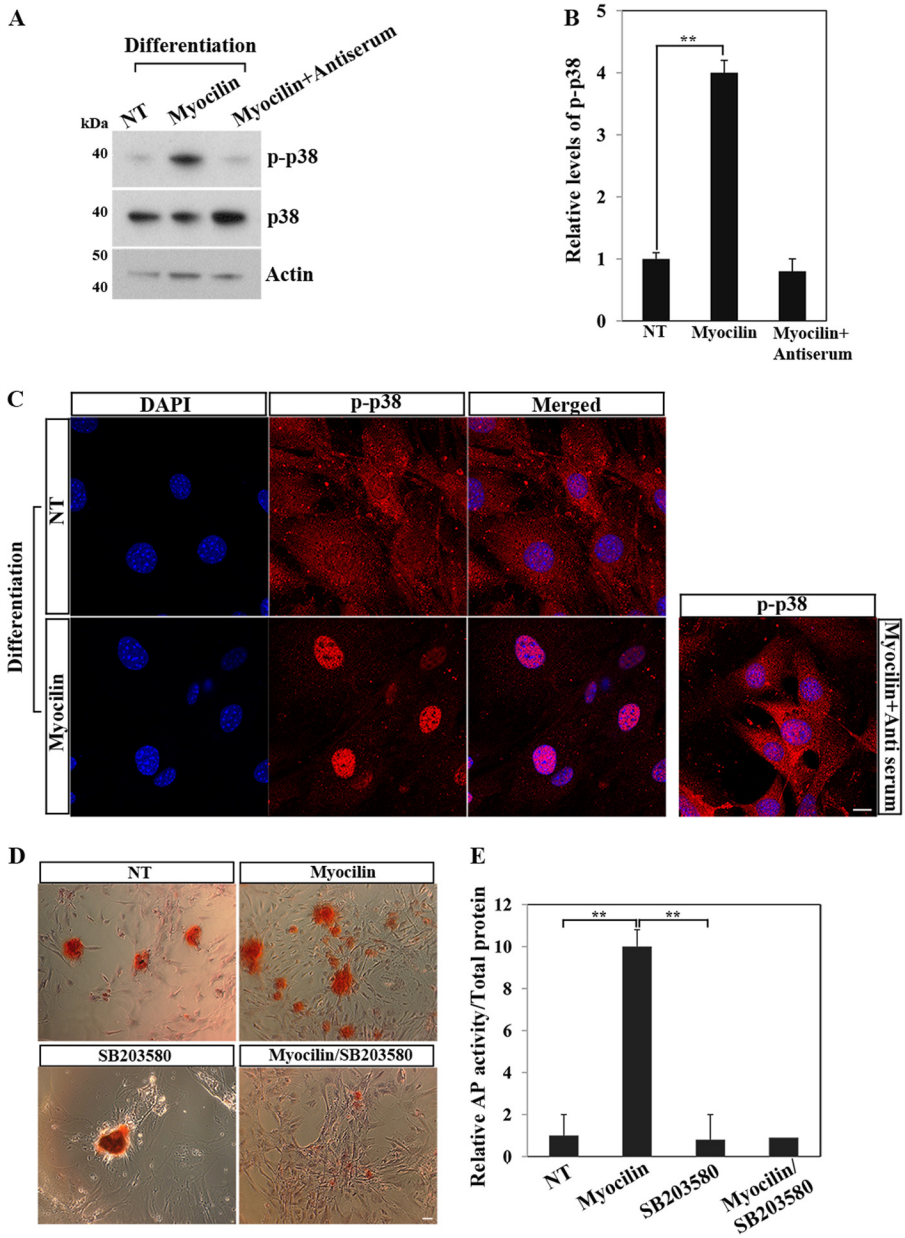

FIGURE 7. **Myocilin-induced activation of the p38 pathway.** *A*, Western blot analysis of phosphorylated p38 (*p-p38*) levels in hMSCs differentiating into osteoblasts for 6 days in the absence (no treatment, *NT*) or presence of myocilin (3 μg/ml). Antiserum against myocilin was added to one sample. *B*, quantification of three independent Western blot experiments with the mean level of p-p38 in hMSC differentiating without myocilin taken as one arbitrary unit. **, $p < 0.01$. *C*, intracellular distribution of p-p38 (*red*) in hMSCs differentiating into osteoblasts in the absence (*NT*) and presence of myocilin (3 μg/ml) for 6 days. Nuclei were stained with DAPI (*blue*). Myocilin antiserum was added where shown. *Scale bar* = 5 μm. *D* and *E*, SB203580 inhibits myocilin-enhanced stimulation of hMSCs into osteoblasts. hMSCs were differentiated into osteoblasts in the absence (*NT*) or presence of myocilin (3 μg/ml). SB203580 (10 μM) was added where shown. Cells were stained with Alizarin Red S. *Scale bar* = 5 μm. Activity of AP was measured in cell lysates and normalized to total protein content. Shown is the quantification of three independent experiments, with the mean level of AP activity in hMSCs differentiating without myocilin taken as one arbitrary unit. **, $p < 0.01$.

etal muscle of *Myoc*-null mice compared with wild-type littermates (13). Data presented in this study show that *Myoc*-null mice exhibit reduced cortical bone thickness and trabecular volume as well as reduced levels of femoral osteopontin. Osteopontin is an abundant non-collagenous sialoprotein in the bone matrix produced by osteoblasts that plays a role their differentiation as well as in bone remodeling (46), osteoclast attachment, and resorption (47).

There is a growing number of cases showing that mutations in interacting proteins may produce similar phenotypes (48). It has been shown that myocilin interacts with sparc (25), a secreted protein that is present in high levels in MSCs and bones (49). MSCs from *sparc*-null mice contain fewer osteoblastic precursors than control mice, and sparc-null osteoblasts are less committed to osteoblastic differentiation than wild-type osteoblasts (50). *Sparc*-null mice show decreased bone mineral density and bone mineral content and increased mechanical fragility of bone (49). Future work should determine whether the biomechanical properties of bones from *Myoc*-null mice are affected similarly.

We have shown that myocilin is expressed in MSCs from different species and that its expression level increases when

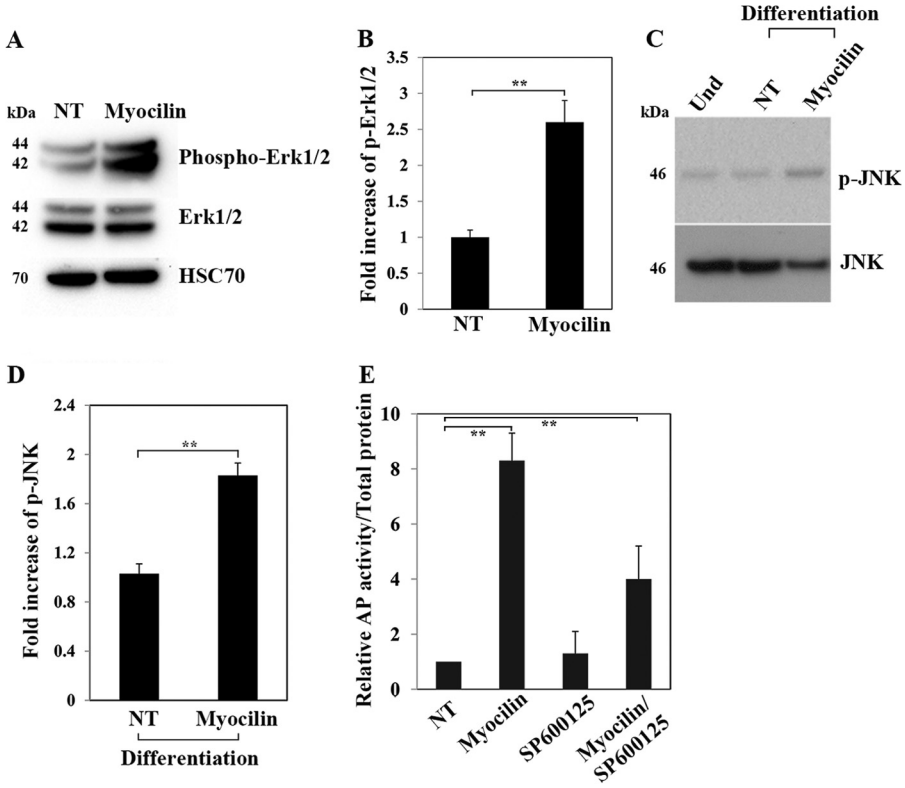

FIGURE 8. **Myocilin-induced activation of the Erk1/2 and JNK pathways.** *A*, Western blot analysis of phosphorylated Erk1/2 (*p-Erk1/2*) levels in hMSCs differentiating into osteoblasts for 6 days in the absence (no treatment, *NT*) or presence of myocilin (3 μg/ml). *B*, quantification of three independent Western blot experiments is shown with the mean level of p-Erk1/2 in hMSC differentiating without myocilin taken as one arbitrary unit. **, $p < 0.01$. *C*, Western blot analysis of phosphorylated JNK (*p-JNK*) levels in undifferentiated hMSCs (*Und*) and hMSCs differentiating into osteoblasts for 6 days in the absence (*NT*) or presence of myocilin (3 μg/ml). *D*, quantification of three independent Western blot experiments with the mean level of p-JNK in hMSC differentiating without myocilin taken as one arbitrary unit. **, $p < 0.01$. *E*, SP600125 (20 μM) inhibits myocilin-enhanced stimulation of hMSCs into osteoblasts. Shown is the quantitation of three independent experiments, with the mean level of AP activity in hMSCs differentiating without myocilin for 6 days taken as one arbitrary unit. **, $p < 0.01$.

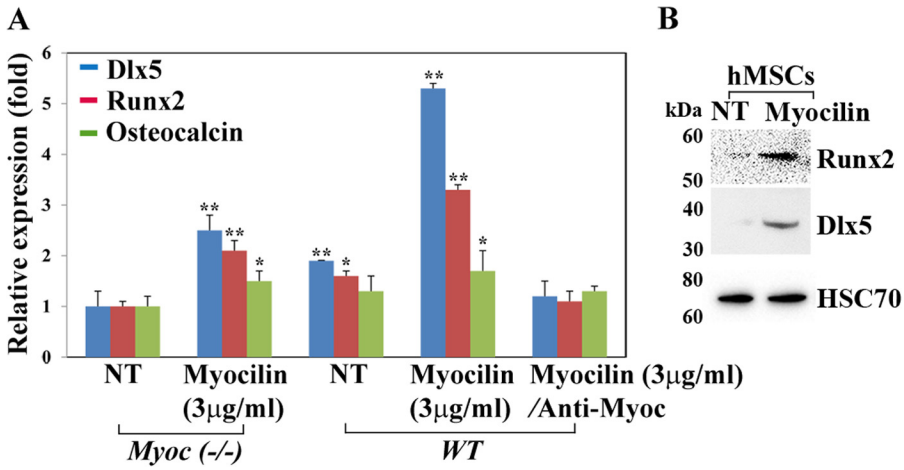

FIGURE 9. **Myocilin-induced changes in the expression of Runx2 and Dlx5 associated with osteoblastic differentiation of MSCs.** *A*, relative levels of indicated mRNAs in mMSCs differentiating into osteoblasts in the absence (no treatment, *NT*) or presence of myocilin (3 μg/ml) for 4 days as judged by qRT-PCR analysis. Antibodies against mouse myocilin were added where shown. GAPDH was used for normalization. The mean levels of indicated mRNAs in mMSCs from *Myoc*-null differentiating in the absence of myocilin were taken as one arbitrary unit. GAPDH mRNA was used for normalization. *, $p < 0.05$; **, $p < 0.01$. *B*, myocilin-induced changes in the level of Runx2 and Dlx5 protein during the course of osteoblastic differentiation of hMSCs (6 days) as judged by Western blot analysis. Equal amounts of lysates were probed with antibodies against Runx2 (1: 1000), Dlx5 (1:1000), and HSC70 (1:2000). These experiments were performed twice, and representative results are shown.

these cells differentiate along the osteoblastic lineage. Although mMSCs express lower levels of myocilin compared with rat MSCs or hMSCs, even these levels of myocilin appear to play a physiological role *in vitro* and *in vivo*. mMSCs from *Myoc*-null mice have a reduced ability to differentiate into the osteoblastic lineage. Addition of extracellular myocilin stimulates differentiation of MSCs along the osteoblastic lineage *in vitro*, and this stimulation includes the activation of the p38, Erk1/2, and, to a

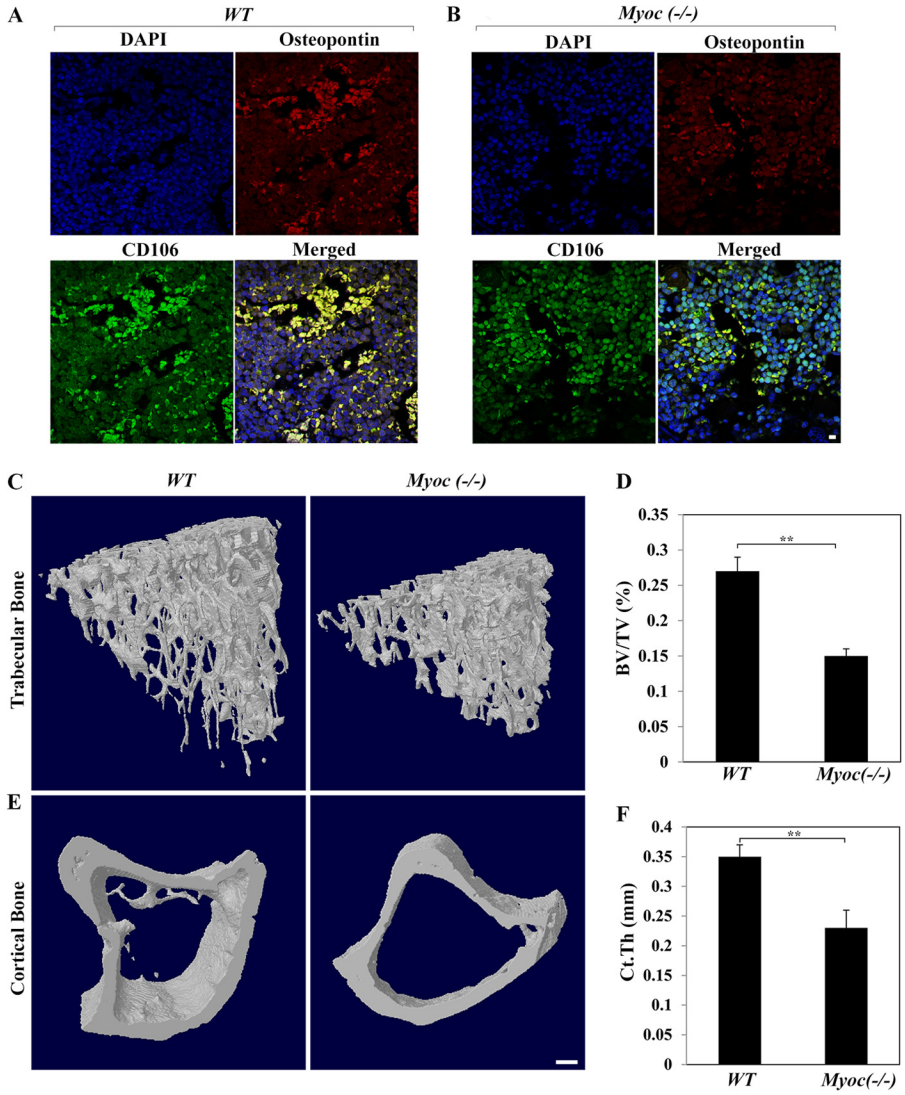

FIGURE 10. **Analysis of bone structure in wild-type and *Myoc*-null mice.** Immunostaining of frozen sections of the femur bone marrow from wild-type (*A*) and *Myoc*-null (*B*) mice with antibodies against osteopontin (1:500) and CD106 (1:500). Nuclei were stained with DAPI. Typical immunofluorescence patterns are shown. *Scale bar* = 10 μm. Representative three-dimensional reconstruction of the trabecular bone (*C*) and cortical bone (*E*) from femurs of 2-month-old wild-type and *Myoc*-null mouse littermates scanned using micro-CT. Micro-CT scans were performed as described under "Experimental Procedures." Three pairs of mice were analyzed. *Scale bar* = 100 μm. Quantitative analyses of the representative three-dimensional reconstructions shown in *C* and *E* are presented in *D* and *F*, respectively. **, $p < 0.01$). *TBV*, trabecular bone volume; *Ct.Th*, midshaft cortical bone thickness.

lesser extent, JNK signaling pathways. It has been shown that the Erk-MAPK pathway plays an important role in Runx2 regulation, osteoblast differentiation, and fetal bone development *in vivo* (51). Activation of p38, but not Erk1/2 or JNK MAPK, and the induction of MSC differentiation into osteoblasts by gold nanoparticles have been reported previously reported (52). At the same time, integrin α5 has been shown to induce osteogenic differentiation of MSCs by activating Erk1/2 but not p38 MAPK (53). After addition of myocilin, similar as in other systems, phosphorylated p38 is translocated into the nucleus where it may phosphorylate Dlx5 and Runx2, resulting in increased transcriptional activity of those factors (54, 55).

It is now well recognized that MSCs may facilitate bone repair and regeneration (56). In particular, MSCs from bone marrow and other sources contribute to bone repair in rodent models (56). MSCs can be introduced therapeutically to sites of regeneration by systemic infusion or via scaffolds loaded with MSCs. Several reports have demonstrated that genetic modification of MSCs (53) or treatment of MSCs with certain growth factors, such as epidermal growth factor (57), before application may accelerate bone repair and regeneration. We have demonstrated that treatment of MSCs with myocilin activates MAPK pathways and accelerates differentiation of these cells onto osteoblasts. Potentially, myocilin may be considered as a potential target that could be employed to improve the bone regenerative potential of MSCs. Moreover, the role that myocilin may play in natural osteogenesis or bone remodeling *in vivo* should be explored further.

Acknowledgment—We thank Danielle Donahue (National Institutes of Health Mouse Imaging Facility) for help with micro-CT scanning and data analysis.

REFERENCES

1. Prockop, D. J., Kota, D. J., Bazhanov, N., and Reger, R. L. (2010) Evolving paradigms for repair of tissues by adult stem/progenitor cells (MSCs). *J. Cell Mol. Med.* **14,** 2190–2199
2. English, K., French, A., and Wood, K. J. (2010) Mesenchymal stromal cells. Facilitators of successful transplantation? *Cell Stem Cell,* **7,** 431–442
3. Caplan, A. I. (2007) Adult mesenchymal stem cells for tissue engineering versus regenerative medicine. *J. Cell Physiol.* **213,** 341–347
4. Pittenger, M. F., Mackay, A. M., Beck, S. C., Jaiswal, R. K., Douglas, R., Mosca, J. D., Moorman, M. A., Simonetti, D. W., Craig, S., and Marshak, D. R. (1999) Multilineage potential of adult human mesenchymal stem cells. *Science* **284,** 143–147
5. Jiang, Y., Jahagirdar, B. N., Reinhardt, R. L., Schwartz, R. E., Keene, C. D., Ortiz-Gonzalez, X. R., Reyes, M., Lenvik, T., Lund, T., Blackstad, M., Du, J., Aldrich, S., Lisberg, A., Low, W. C., Largaespada, D. A., and Verfaillie, C. M. (2002) Pluripotency of mesenchymal stem cells derived from adult marrow. *Nature* **418,** 41–49
6. Kratchmarova, I., Blagoev, B., Haack-Sorensen, M., Kassem, M., and Mann, M. (2005) Mechanism of divergent growth factor effects in mesenchymal stem cell differentiation. *Science* **308,** 1472–1477
7. Lin, G. L., and Hankenson, K. D. (2011) Integration of BMP, Wnt, and Notch signaling pathways in osteoblast differentiation. *J. Cell Biochem.* **112,** 3491–3501
8. Fingert, J. H., Héon, E., Liebmann, J. M., Yamamoto, T., Craig, J. E., Rait, J., Kawase, K., Hoh, S. T., Buys, Y. M., Dickinson, J., Hockey R. R., Williams-Lyn, D., Trope, G., Kitazawa, Y., Ritch, R., Mackey, D. A., Alward, W. L., Sheffield, V. C., and Stone, E. M. (1999) Analysis of myocilin mutations in 1703 glaucoma patients from five different populations. *Hum. Mol. Genet.* **8,** 899–905
9. Fingert, J. H., Stone, E. M., Sheffield, V. C., and Alward, W. L. (2002) Myocilin glaucoma. *Surv. Ophthalmol.* **47,** 547–561
10. Stone, E. M., Fingert, J. H., Alward, W. L., Nguyen, T. D., Polansky, J. R., Sunden, S. L., Nishimura, D., Clark, A. F., Nystuen, A., Nichols, B. E., Mackey, D. A., Ritch, R., Kalenak, J. W., Craven, E. R., and Sheffield, V. C. (1997) Identification of a gene that causes primary open angle glaucoma. *Science* **275,** 668–670
11. Kwon, Y. H., Fingert, J. H., Kuehn, M. H., and Alward, W. L. (2009) Primary open-angle glaucoma. *N. Engl. J. Med.* **360,** 1113–1124
12. Adam, M. F., Belmouden, A., Binisti, P., Brézin, A. P., Valtot, F., Béchetoille, A., Dascotte, J. C., Copin, B., Gomez, L., Chaventré, A., Bach, J. F., and Garchon, H. J. (1997) Recurrent mutations in a single exon encoding the evolutionarily conserved olfactomedin-homology domain of TIGR in familial open-angle glaucoma. *Hum. Mol. Genet.* **6,** 2091–2097
13. Joe, M. K., Kee, C., and Tomarev, S. I. (2012) Myocilin interacts with syntrophins and is member of dystrophin-associated protein complex. *J. Biol. Chem.* **287,** 13216–13227
14. Kwon, H. S., Lee, H. S., Ji, Y., Rubin, J. S., and Tomarev, S. I. (2009) Myocilin is a modulator of Wnt signaling. *Mol. Cell. Biol.* **29,** 2139–2154
15. Kim, B. S., Savinova, O. V., Reedy, M. V., Martin, J., Lun, Y., Gan, L., Smith, R. S., Tomarev, S. I., John, S. W., and Johnson, R. L. (2001) Targeted disruption of the myocilin gene (Myoc) suggests that human glaucoma-causing mutations are gain of function. *Mol. Cell. Biol.* **21,** 7707–7713
16. Johnson, T. V., Bull, N. D., Hunt, D. P., Marina, N., Tomarev, S. I., and Martin, K. R. (2010) Neuroprotective effects of intravitreal mesenchymal stem cell transplantation in experimental glaucoma. *Invest. Ophthalmol. Vis. Sci.* **51,** 2051–2059
17. Soleimani, M., and Nadri, S. (2009) A protocol for isolation and culture of mesenchymal stem cells from mouse bone marrow. *Nat. Protoc.* **4,** 102–106
18. Malyukova, I., Lee, H. S., Fariss, R. N., and Tomarev, S. I. (2006) Mutated mouse and human myocilins have similar properties and do not block general secretory pathway. *Invest. Ophthalmol. Vis. Sci.* **47,** 206–212
19. Johnstone, B., Hering, T. M., Caplan, A. I., Goldberg, V. M., and Yoo, J. U. (1998) *In vitro* chondrogenesis of bone marrow-derived mesenchymal progenitor cells. *Exp. Cell Res.* **238,** 265–272
20. Mackay, A. M., Beck, S. C., Murphy, J. M., Barry, F. P., Chichester, C. O., and Pittenger, M. F. (1998) Chondrogenic differentiation of cultured human mesenchymal stem cells from marrow. *Tissue Eng.* **4,** 415–428
21. Tomarev, S. I., Tamm, E. R., and Chang, B. (1998) Characterization of the mouse Myoc/Tigr gene. *Biochem. Biophys. Res. Comm.* **245,** 887–893
22. O'Brien, E. T., Ren, X., and Wang, Y. (2000) Localization of myocilin to the Golgi apparatus in Schlemm's canal cells. *Invest. Ophthalmol. Vis. Sci.* **41,** 3842–3849
23. Nguyen, T. D., Chen, P., Huang, W. D., Chen, H., Johnson, D., and Polansky, J. R. (1998) Gene structure and properties of TIGR, an olfactomedin-related glycoprotein cloned from glucocorticoid-induced trabecular meshwork cells. *J. Biol. Chem.* **273,** 6341–6350
24. Shepard, A. R., Jacobson, N., Fingert, J. H., Stone, E. M., Sheffield, V. C., and Clark, A. F. (2001) Delayed secondary glucocorticoid responsiveness of MYOC in human trabecular meshwork cells. *Invest. Ophthalmol. Vis. Sci.* **42,** 3173–3181
25. Aroca-Aguilar, J. D., Sánchez-Sánchez, F., Ghosh, S., Fernández-Navarro, A., Coca-Prados, M., and Escribano, J. (2011) Interaction of recombinant myocilin with the matricellular protein SPARC. Functional implications. *Invest. Ophthalmol. Vis. Sci.* **52,** 179–189
26. Peters, D. M., Herbert, K., Biddick, B., and Peterson, J. A. (2005) Myocilin binding to Hep II domain of fibronectin inhibits cell spreading and incorporation of paxillin into focal adhesions. *Exp. Cell Res.* **303,** 218–228
27. Lemonnier, J., Ghayor, C., Guicheux, J., and Caverzasio, J. (2004) Protein kinase C-independent activation of protein kinase D is involved in BMP-2-induced activation of stress mitogen-activated protein kinases JNK and p38 and osteoblastic cell differentiation. *J. Biol. Chem.* **279,** 259–264
28. Celil, A. B., and Campbell, P. G. (2005) BMP-2 and insulin-like growth factor-I mediate Osterix (Osx) expression in human mesenchymal stem cells via the MAPK and protein kinase D signaling pathways. *J. Biol. Chem.* **280,** 31353–31359
29. Lee, J. C., Laydon, J. T., McDonnell, P. C., Gallagher, T. F., Kumar, S., Green, D., McNulty, D., Blumenthal, M. J., Heys, J. R., and Landvatter, S. W. (1994) A protein kinase involved in the regulation of inflammatory cytokine biosynthesis. *Nature* **372,** 739–746
30. Cuenda, A., and Rousseau, S. (2007) p38 MAP-kinases pathway regulation, function and role in human diseases. *Biochim. Biophys. Acta* **1773,** 1358–1375
31. Bogoyevitch, M. A., and Arthur, P. G. (2008) Inhibitors of c-Jun N-terminal kinases. JuNK no more? *Biochim. Biophys. Acta* **1784,** 76–93
32. Bain, J., Plater, L., Elliott, M., Shpiro, N., Hastie, C. J., McLauchlan, H., Klevernic, I., Arthur, J. S., Alessi, D. R., and Cohen, P. (2007) The selectivity of protein kinase inhibitors. A further update. *Biochem. J.* **408,** 297–315
33. Pargellis, C., Tong, L., Churchill, L., Cirillo, P. F., Gilmore, T., Graham, A. G., Grob, P. M., Hickey, E. R., Moss, N., Pav, S., and Regan, J. (2002) Inhibition of p38 MAP kinase by utilizing a novel allosteric binding site. *Nat. Struct. Biol.* **9,** 268–272
34. Stebbins, J. L., De, S. K., Machleidt, T., Becattini, B., Vazquez, J., Kuntzen, C., Chen, L. H., Cellitti, J. F., Riel-Mehan, M., Emdadi, A., Solinas, G., Karin, M., and Pellecchia, M. (2008) Identification of a new JNK inhibitor targeting the JNK-JIP interaction site. *Proc. Natl. Acad. Sci. U.S.A.* **105,** 16809–16813
35. Gordeladze, J. O., Noël, D., Bony, C., Apparailly, F., Louis-Plence, P., and Jorgensen, C. (2008) Transient down-regulation of cbfa1/Runx2 by RNA interference in murine C3H10T1/2 mesenchymal stromal cells delays *in vitro* and *in vivo* osteogenesis, but does not overtly affect chondrogenesis. *Exp. Cell Res.* **314,** 1495–1506
36. Lee, M. H., Kwon, T. G., Park, H. S., Wozney, J. M., and Ryoo, H. M. (2003) BMP-2-induced Osterix expression is mediated by Dlx5 but is independent of Runx2. *Biochem. Biophys. Res. Comm.* **309,** 689–694
37. Gonzalez, P., Epstein, D. L., and Borrás, T. (2000) Characterization of gene expression in human trabecular meshwork using single-pass sequencing of 1060 clones. *Invest. Ophthalmol. Vis. Sci.* **41,** 3678–3693
38. Tomarev, S. I., Wistow, G., Raymond, V., Dubois, S., and Malyukova, I. (2003) Gene expression profile of the human trabecular meshwork. NEIBank sequence tag analysis. *Invest. Ophthalmol. Vis. Sci.* **44,** 2588–2596
39. Borrás, T., and Comes, N. (2009) Evidence for a calcification process in the trabecular meshwork. *Exp. Eye Res.* **88,** 738–746
40. Joe, M. K., and Tomarev, S. I. (2010) Expression of myocilin mutants

sensitizes cells to oxidative stress-induced apoptosis. Implication for glaucoma pathogenesis. *Am. J. Pathol.* **176,** 2880–2890
41. Joe, M. K., Sohn, S., Hur, W., Moon, Y., Choi, Y. R., and Kee, C. (2003) Accumulation of mutant myocilins in ER leads to ER stress and potential cytotoxicity in human trabecular meshwork cells. *Biochem. Biophys. Res. Comm.* **312,** 592–600
42. Zode, G. S., Kuehn, M. H., Nishimura, D. Y., Searby, C. C., Mohan, K., Grozdanic, S. D., Bugge, K., Anderson, M. G., Clark, A. F., Stone, E. M., and Sheffield, V. C. (2011) Reduction of ER stress via a chemical chaperone prevents disease phenotypes in a mouse model of primary open angle glaucoma. *J. Clin. Invest.* **121,** 3542–3553
43. Zhou, Y., Grinchuk, O., and Tomarev, S. I. (2008) Transgenic mice expressing the Tyr-437His mutant of human myocilin protein develop glaucoma. *Invest. Ophthalmol. Vis. Sci.* **49,** 1932–1939
44. Senatorov, V., Malyukova, I., Fariss, R., Wawrousek, E. F., Swaminathan, S., Sharan, S. K., and Tomarev, S. (2006) Expression of mutated mouse myocilin induces open-angle glaucoma in transgenic mice. *J. Neurosci.* **26,** 11903–11914
45. Gould, D. B., Reedy, M., Wilson, L. A., Smith, R. S., Johnson, R. L., and John, S. W. (2006) Mutant myocilin nonsecretion *in vivo* is not sufficient to cause glaucoma. *Mol. Cell. Biol.* **26,** 8427–8436
46. Choi, S. T., Kim, J. H., Kang, E. J., Lee, S. W., Park, M. C., Park, Y. B., and Lee, S. K. (2008) Osteopontin might be involved in bone remodelling rather than in inflammation in ankylosing spondylitis. *Rheumatology* **47,** 1775–1779
47. Sodek, J., Ganss, B., and McKee, M. D. (2000) *Osteopontin. Crit. Rev. Oral Biol. Med.* **11,** 279–303
48. Oti, M., Snel, B., Huynen, M. A., and Brunner, H. G. (2006) Predicting disease genes using protein-protein interactions. *J. Med. Genet.* **43,** 691–698
49. Delany, A. M., and Hankenson, K. D. (2009) Thrombospondin-2 and SPARC/osteonectin are critical regulators of bone remodeling. *J. Cell Comm. Signaling* **3,** 227–238
50. Delany, A. M., Kalajzic, I., Bradshaw, A. D., Sage, E. H., and Canalis, E. (2003) Osteonectin-null mutation compromises osteoblast formation, maturation, and survival. *Endocrinol.* **144,** 2588–2596
51. Ge, C., Xiao, G., Jiang, D., and Franceschi, R. T. (2007) Critical role of the extracellular signal-regulated kinase-MAPK pathway in osteoblast differentiation and skeletal development. *J. Cell Biol.* **176,** 709–718
52. Yi, C., Liu, D., Fong, C. C., Zhang, J., and Yang, M. (2010) Gold nanoparticles promote osteogenic differentiation of mesenchymal stem cells through p38 MAPK pathway. *ACS Nano,* **4,** 6439–6448
53. Hamidouche, Z., Fromigué, O., Ringe, J., Häupl, T., Vaudin, P., Pagès, J. C., Srouji, S., Livne, E., and Marie, P. J. (2009) Priming integrin α5 promotes human mesenchymal stromal cell osteoblast differentiation and osteogenesis. *Proc. Natl. Acad. Sci. U.S.A.* **106,** 18587–18591
54. Ulsamer, A., Ortuño, M. J., Ruiz, S., Susperregui, A. R., Osses, N., Rosa, J. L., and Ventura, F. (2008) BMP-2 induces Osterix expression through up-regulation of Dlx5 and its phosphorylation by p38. *J. Biol. Chem.* **283,** 3816–3826
55. Greenblatt, M. B., Shim, J. H., Zou, W., Sitara, D., Schweitzer, M., Hu, D., Lotinun, S., Sano, Y., Baron, R., Park, J. M., Arthur, S., Xie, M., Schneider, M. D., Zhai, B., Gygi, S., Davis, R., and Glimcher, L. H. (2010) The p38 MAPK pathway is essential for skeletogenesis and bone homeostasis in mice. *J. Clin. Invest.* **120,** 2457–2473
56. Griffin, M., Iqbal, S. A., and Bayat, A. (2011) Exploring the application of mesenchymal stem cells in bone repair and regeneration. *J. Bone Joint Surg. Br.* **93,** 427–434
57. Tamama, K., Kawasaki, H., and Wells, A. (2010) Epidermal growth factor (EGF) treatment on multipotential stromal cells (MSCs). Possible enhancement of therapeutic potential of MSC. *J. Biomed. Biotechnol.* **2010,** 795385